

Research Article

A Comparative Study of Solvothermal and Sol-Gel-Derived Nanocrystalline Alumina Catalysts for Ethanol Dehydration

Mingkwan Wannaborworn, Piyasan Prasertdam, and Bunjerd Jongsomjit

Center of Excellence on Catalysis and Catalytic Reaction Engineering, Department of Chemical Engineering, Faculty of Engineering, Chulalongkorn University, Bangkok 10330, Thailand

Correspondence should be addressed to Bunjerd Jongsomjit; bunjerd.j@chula.ac.th

Received 6 August 2015; Revised 2 November 2015; Accepted 12 November 2015

Academic Editor: Antonios Kelarakis

Copyright © 2015 Mingkwan Wannaborworn et al. This is an open access article distributed under the Creative Commons Attribution License, which permits unrestricted use, distribution, and reproduction in any medium, provided the original work is properly cited.

The ethanol dehydration to ethylene over alumina catalysts prepared by solvothermal and sol-gel methods was investigated. Also, a commercial alumina was used for comparison purposes. The results showed that the catalytic activity depends on the properties of catalyst derived from different preparation methods and reaction temperature. The alumina synthesized by solvothermal method exhibited the highest activity. This can be attributed to the higher surface area and larger amount of acid site, especially the ratio of weak/strong acid strength as determined by N_2 physisorption and NH_3 -TPD studies. The solvothermal-derived catalyst exhibited an excellent performance with complete ethanol conversion and 100% selectivity to ethylene at $350^\circ C$ in comparison with other ones. In addition, we further studied the catalytic dehydration of alumina catalyst modified with Fe. The presence of 10 wt.% Fe decreased both conversion and ethylene selectivity. However, the acetaldehyde selectivity apparently increased. It was related to the dehydrogenation pathway that takes place on Fe species.

1. Introduction

Nowadays, ethylene is one of the most important compounds for the petrochemical industry. It has been used as feedstock to produce many products such as polyethylene, polystyrene, vinyl chloride, and ethylene oxide, and, therefore, the global demand for ethylene is expected to increase with the continuous increasing of crude oil price [1, 2]. Ethylene is conventionally produced by thermal cracking of petroleum or natural gas. Since this process requires high temperature (750 – $900^\circ C$) and the natural resource is limited, much attention has been paid to find the alternative approach to produce ethylene. Recent studies have shown that one effective route by using biomass, especially bioethanol, is considered as the most promising way instead of using petroleum as feedstock. The ethanol dehydration provides many advantages such as lower operating temperature and green manufacturing of ethylene. Hence, the development of dehydration performance has been widely studied in both industry and academia [3–7]. The catalysts most commonly used for ethanol to ethylene are based on zeolite [8, 9], alumina [10, 11],

silica [12], and silica-alumina [13]. For HZM-5 zeolites, these catalysts possess smaller pore size and have high acid strength. Their properties cause coke deposition resulting in the deactivation of catalyst, so zeolites are inappropriate for dehydration [14, 15]. Among them, alumina is found as an efficient catalyst because of its high specific surface area, excellent thermal stability, and wide range of chemical properties, especially lower acid strength than zeolites [15, 16]. It is thus the most common catalyst used to produce ethylene.

Although several studies have been investigated on the relationship between the catalyst structures and performances in ethanol dehydration, an understanding on how the textural properties of catalyst would affect the catalytic activity has not yet been reached. Hosseini and Nikou [17] synthesized γ -alumina by coprecipitation method with four precipitants and used it as a catalyst for methanol dehydration. The results showed that catalyst prepared by ammonium carbonate showed higher catalytic activity compared to commercial catalyst despite having lower amount of acid sites. The high activity is related to the high surface area and pore volume of catalyst. Akarmazyan et al. [18]

investigated the methanol dehydration to dimethyl ether over commercial alumina with different physicochemical characteristics and found that the catalyst with smaller crystallite size exhibited higher catalytic activity, and it could be due to its large external surface area, thus facilitating reaction between reactant and active site. Therefore, the textural properties are important factors that need to be considered. In addition, many efforts have been made to improve the dehydration performance by adding some dopants such as titania, niobia, molybdenum oxide, and silica. Chen et al. [5] pointed out that an addition of TiO_2 onto alumina enhanced the ethanol conversion and ethylene selectivity. The yield of ethylene as high as 98.3% could be achieved for 10 wt.% $\text{TiO}_2/\text{Al}_2\text{O}_3$ catalysts at 440°C . The higher catalytic activity was consistent with the higher amount of moderate acid sites. Liu et al. [19] studied the dehydration of methanol to DME over modified $\gamma\text{-Al}_2\text{O}_3$ catalysts. Results showed that Nb_2O_5 contents significantly affect the catalytic performance of catalysts. The 10 wt.% of Nb_2O_5 exhibited the highest activity in the low temperature due to its largest surface area. In another work by Yaripour et al. [20], the SiO_2 modification showed a promising way to increase a catalytic activity. Both yield and selectivity were the highest at 2 wt.% of silica, which was attributed to high surface area and high surface acidity, especially the highest weak to moderate acid site.

Recently, many investigations have been paid attention on the utilization of supported Fe catalysts. It is well known that Fe catalyst is active and often used in some important processes such as the catalytic decomposition of N_2O [21], conversion of natural gas to syn-gas [22], and the propane oxidative dehydrogenation [23]. So, in this work, we extend our study on how the Fe-modified alumina catalyst affects the catalytic activity for ethanol dehydration.

In this study, the catalytic activity of alumina catalyst prepared by solvothermal and sol-gel methods as well as commercial alumina for ethanol dehydration was investigated. The catalysts were characterized by means of XRD, N_2 physisorption, SEM/EDX, and NH_3 -TPD analyses.

2. Experimental

2.1. Catalyst Preparation. Alumina catalysts were synthesized according to the procedure reported previously [24, 25] and is described below.

2.1.1. Solvothermal Method. An amount of 25 g of aluminium isopropoxide (AIP) as a starting material was suspended in 100 mL of 1-butanol in a test tube and then placed in an autoclave. In the gap between the autoclave wall and test tube, 30 mL of 1-butanol was added. The autoclave was purged with nitrogen gas before heating up to 300°C and held at that temperature for 2 h. After the autoclave was cooled down to room temperature, the obtained powder was washed with methanol followed by centrifugation. Finally, the white powder product was dried at 120°C for 24 h and calcined in air at 600°C for 6 h.

2.1.2. Sol-Gel Method. The same volume of ethanol and deionized water was added to the flask. The solution was stirred under 20 rpm/min and heated to 80°C . After the solution was kept for 1 h, 15 g aluminum isopropoxide used as a precursor was added to the solution under continuous stirring. The hydrolysis step was carried out at 80°C by adding a certain volume of 10 M HCl (37%). The mixture was stirred at that temperature for 8 h. The obtained product was dried at 115°C for 24 h and further calcined in air at 550°C for 6 h to obtain white alumina catalyst.

2.2. Ethanol Dehydration Reaction. Dehydration of ethanol to ethylene was conducted in a glass fixed-bed reactor (length = 0.33 m and inner diameter = 7 mm). A glass reactor was placed into a temperature-programmed tubular furnace. All experiments were performed under atmospheric pressure and in the temperature range 200 to 400°C using a feed composition consisting of 99.95% ethanol. In a typical run, 0.05 g of alumina catalysts obtained from Sections 2.1.1 and 2.1.2 and commercial alumina (Fluka) was charged into the middle zone of reactor tube and pure ethanol as feed was stored in vaporizer. Prior to testing, the catalysts were activated at 200°C for 1 h under an argon gas flow. Ethanol was conveyed into reactor at an argon gas flow rate of 50 mL/min. The reaction was carried out at each temperature for 1 h. The dehydration products were analyzed by a gas chromatography (Shimadzu GC-14A) with a FID detector using DB-5 capillary column.

2.3. Catalyst Characterization

2.3.1. X-Ray Diffraction (XRD). XRD was used to study the bulk crystalline phase of samples. The XRD pattern was performed by SIEMENS D5000 X-ray diffractometer with CuK_α radiation. Those samples were scanned in the range of $2\theta = 10\text{--}90$.

2.3.2. N_2 -Physisorption. The surface area and average pore volume of prepared catalysts were determined by Micromeritics ChemiSorb 2750 Pulse instrument. Measurement was performed at -196°C and calculated according to the BET isotherm equation.

2.3.3. Scanning Electron Microscopy (SEM) and Energy Dispersive X-Ray Spectroscopy (EDX). Hitachi S-3400N model was used to determine the catalyst morphology. Their elemental distribution and composition over different catalysts were performed by Link Isis Series 300 program EDX.

2.3.4. Ammonia Temperature-Programmed Desorption (NH_3 -TPD). The acid properties of all catalysts were determined by using Micromeritics ChemiSorb 2750 Pulse Chemisorption System. Under a helium gas flow, the Fe-modified and unmodified catalysts were pretreated at 550°C for 1 h. Then, the catalyst was saturated with 15% NH_3/He at 40°C for 30 min. After chemisorption step, a helium gas was flown over catalyst to remove any adsorbed molecules from catalyst active site from temperature of 40 to 500°C at heating rate

TABLE 1: Physical properties of alumina catalysts prepared by different methods.

Catalyst	Surface area (m ² /g)	Pore volume (cm ³ /g)	Pore diameter (nm)	Crystallite size (nm) ^a
Al-SV	215	0.770	9.33	3.78
Al-SG	152	0.221	3.46	4.78
Al-com	137	0.212	3.88	5.62

^aCrystallite size of alumina: determined by XRD results using Scherrer equation.

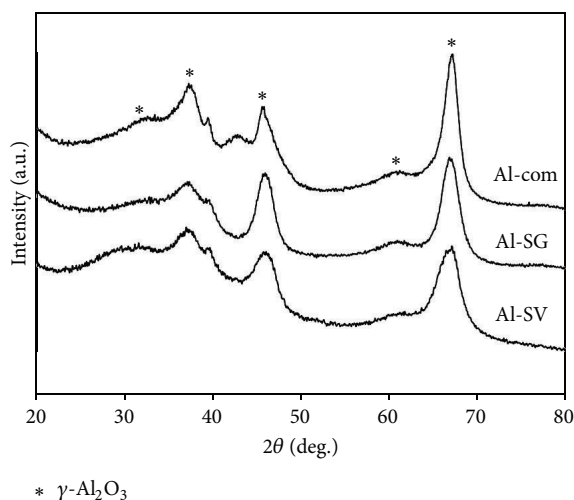


FIGURE 1: XRD patterns of different catalysts.

10°C/min. The NH₃ TPD profile is a plot of the TCD signal as a function of temperature to report the amount of ammonia, which is related to catalyst acidity.

2.3.5. Thermogravimetric Analysis (TGA). TGA was performed using a TA Instrument SDT Q600 analyzer (USA). The samples of 10–20 mg and a temperature range between 30 and 400°C at 2°C min⁻¹ were used in the operation with N₂ UHP carrier gas.

3. Results and Discussion

3.1. Catalyst Characterization. The XRD patterns of all samples are shown in Figure 1. It can be seen that the characteristic peaks at $2\theta = 37, 46, 61,$ and 67 indicating typically γ -phase of alumina [18, 33]. The XRD pattern of alumina synthesized by solvothermal (Al-SV) method was broad, because the crystallite sizes were very small, while the catalyst prepared by sol-gel method (Al-SG) and commercial alumina (Al-com) exhibited sharp peaks due to the presence of large crystallite size. The average crystallite size of the catalysts was calculated using Scherrer equation and shown in Table 1. The average crystallite size of alumina prepared by solvothermal method (Al-SV) was the smallest.

Figure 2 shows the nitrogen adsorption/desorption isotherms of alumina catalysts. All samples exhibited type IV isotherms, indicating they are mesoporous materials. For Al-SV, the sample presented hysteresis loop of type H1, occurring at higher relative pressure ($P/P_0 = 0.7$ to 0.9) compared with

other catalysts. It indicates larger mesopores and broad pore size distribution with uniform cylindrical shapes. Meanwhile, the isotherm for sol-gel-derived catalyst showed quite different pattern. Two inflection points and hysteresis loop moved toward lower pressure were observed. This suggests that lower porosity and cylindrical mesopores were expected for Al-SG. For Al-com, the isotherm was similar to that for Al-SG, but with slightly decreased BET surface area and pore volume [18, 34]. The observations are consistent with the value of surface area and sample porosity as shown in Table 1, in which the pore volume of Al-SV, Al-SG, and Al-com was 0.770, 0.221, and 0.212 cm³/g, respectively. The surface area of Al-SV was the highest, while the Al-com had the lowest surface area. Also, it was in accordance with those obtained from XRD analysis, where the samples with smaller crystallites exhibit higher surface area. The catalyst with small crystallite size may possess higher catalytic activity, because more active sites on large external surface area are easily reacted with reactants [18].

The pore size distribution (PSD) calculated by BJH method is shown in Figure 3. The Al-SV sample exhibited a bimodal pore size distribution, where pore diameter was in the ranges of 7–9 nm and 23–25 nm. For Al-SG and Al-com catalysts, the samples have a narrow pore size distribution with an average pore diameter around 3 nm, confirming the pore size distribution in the mesoporous range. It can be seen that the calculated pore size distribution was in good agreement with N₂ isotherm as mentioned above. This finding suggests the difference in porous nature greatly affected by preparation method (sol-gel and solvothermal).

To examine the catalyst morphology, SEM technique was performed. The SEM micrographs of different catalysts are shown in Figure 4. For those catalysts synthesized by solvothermal method, agglomeration of primary particles exhibited the porous shape, where the Al-SG and Al-com catalysts consisted of agglomerated particles with primarily irregular shape. The proposed different morphology of alumina obtained from the solvothermal and sol-gel methods is illustrated in Scheme 1.

Considering the distribution of surface acidity and the strength of acid sites in different alumina catalysts, NH₃-TPD was examined. Although NH₃-TPD technique has some drawbacks [1], it is fast, simple, and frequently employed method to evaluate the catalyst acidity. The typical NH₃-TPD profile for catalysts is shown in Figure 5. It can be seen that there were two types of acidic sites for Al-SV, Al-SG, and Al-com. The first peak observed at lower temperature ($\approx 250^\circ\text{C}$) was due to the desorption of ammonia chemisorbed at the weak to moderate acid sites, while the higher temperature peak centered at 400°C was related to the acid site with high

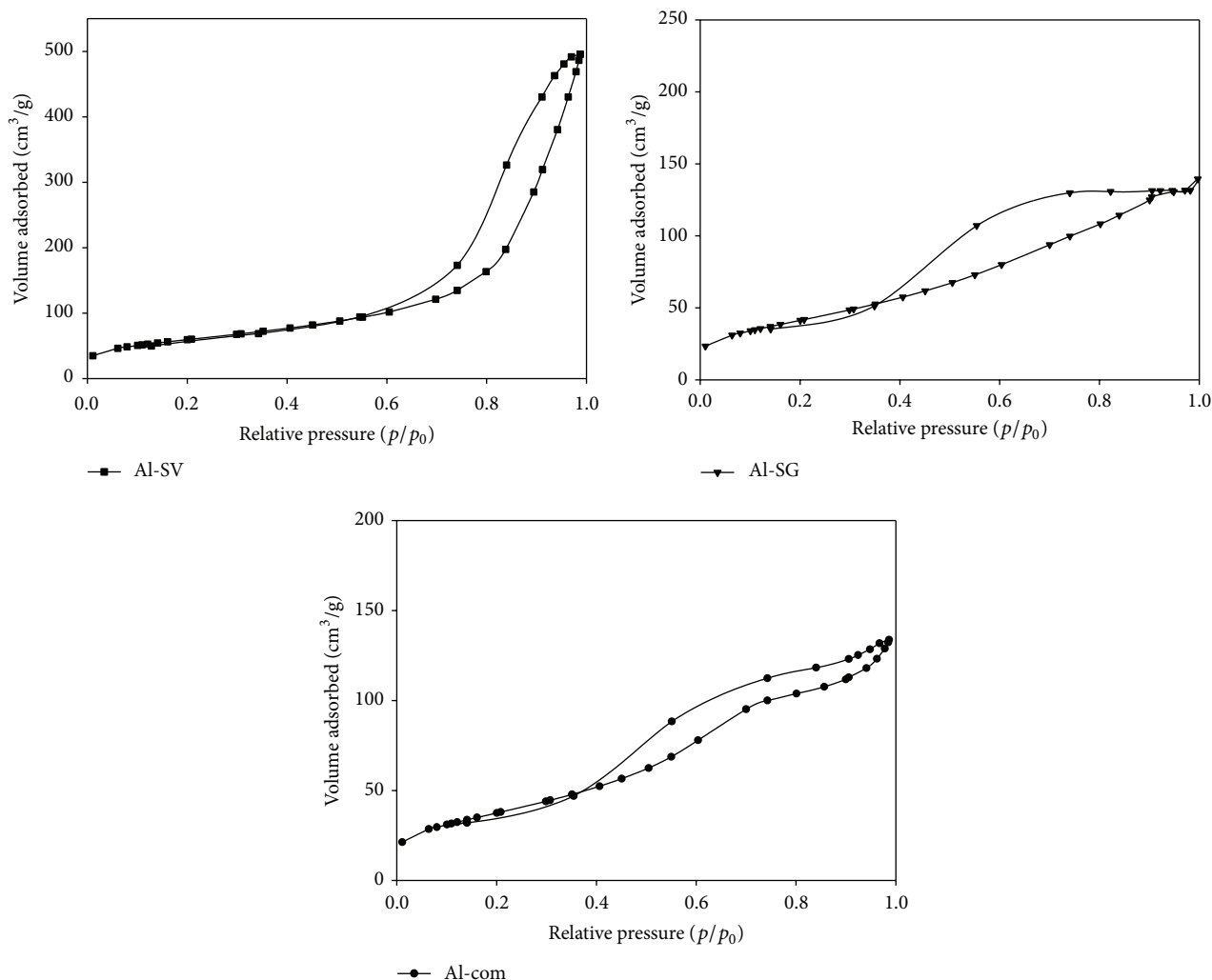


FIGURE 2: Nitrogen adsorption/desorption isotherms of different alumina catalysts.

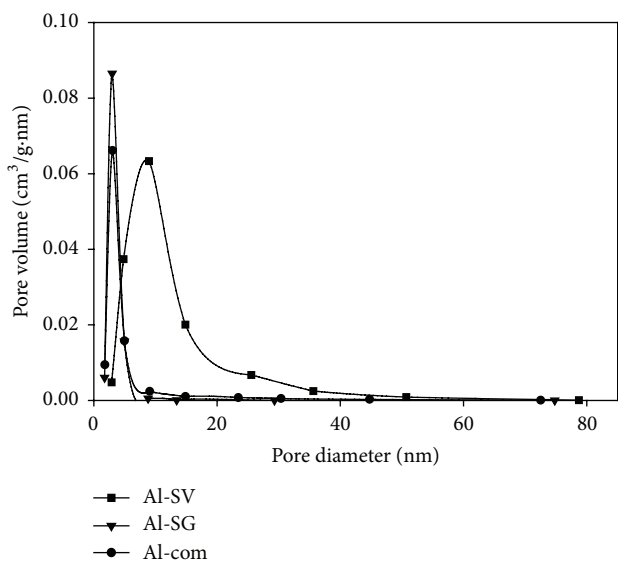


FIGURE 3: BJH pore size distribution of different alumina catalysts.

strength [35]. The amount of acid sites was determined from NH_3 -TPD curve by deconvolution according to the Gauss curve fitting method. The results are provided in Table 2, which demonstrated that the amount of strong acid site was higher than weak to moderate acid sites for all catalysts. The Al-SV has the highest amount of weak to moderate acid sites compared to Al-SG and Al-com. According to Chen et al. [5], higher ethylene selectivity of $\text{TiO}_2/\gamma\text{-Al}_2\text{O}_3$ catalysts is consistent with the higher acidity. Thus, the difference in catalytic performance of these catalysts depending on the acid amount will be discussed further.

3.2. Catalytic Performance of Ethanol Dehydration

Effect of Reaction Temperatures. In order to study the effect of reaction temperatures on the conversion of ethanol and selectivities to ethylene, diethyl ether, and acetaldehyde, the dehydration was examined over the Al-SV catalyst in the temperature range from 200 to 400°C. As known, the product distribution of ethanol dehydration strongly depends on

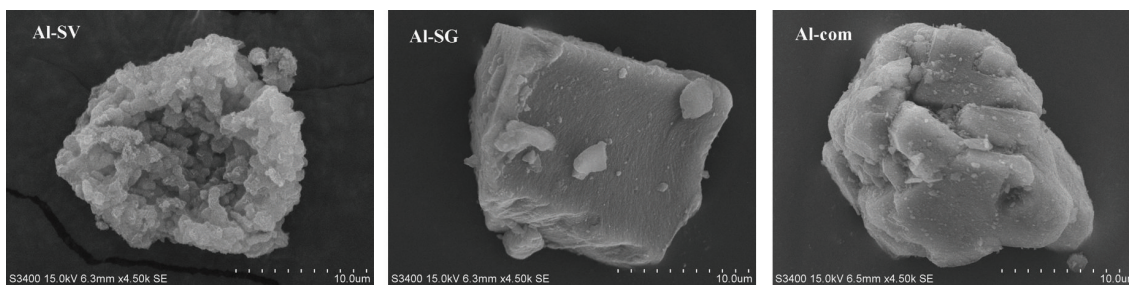
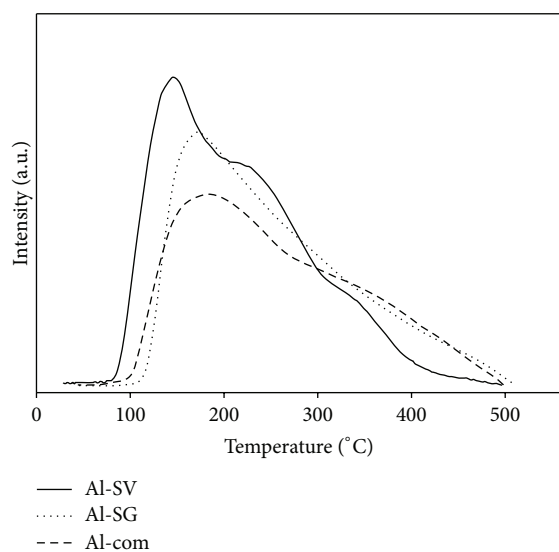


FIGURE 4: SEM images of different catalysts.

FIGURE 5: NH_3 -TPD profile of the different alumina catalysts.TABLE 2: NH_3 -TPD results of different alumina catalysts.

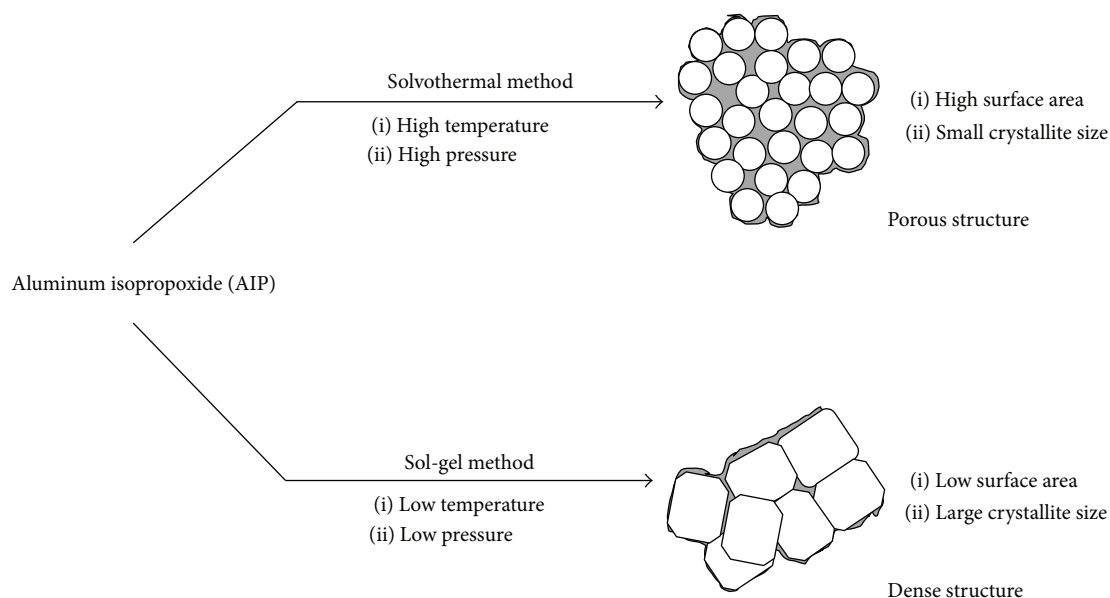
Catalyst	Number of acid sites ($\mu\text{mol NH}_3/\text{g catalyst}$)			Total
	Weak to moderate	Strong	Weak/strong	
Al-SV	360	441	0.82	801
Al-SG	235	386	0.61	621
Al-com	256	442	0.58	698

the reaction temperatures. Low temperatures favor the diethyl ether production, while the ethylene formation occurs at high temperature. It is evident from Figure 6 that the conversion increased with an increase in the reaction temperature. The Al-SV exhibited the highest conversion and ethylene selectivity of 100% at 350°C and kept constant at 400°C. The enhanced catalytic activity is related to the reaction pathway. Generally, for ethylene production through ethanol dehydration, there are two competitive pathways during reaction. The main path involves the formation of ethylene. This reaction occurring via intramolecular is endothermic. The second one, inter-molecular dehydration to diethyl ether, is exothermic [5, 15, 26]. The results of activity test in Figure 6 show that when increasing the reaction temperature, the selectivity to ethylene continuously increased,

whereas the decrease in diethyl ether selectivity was evident over selected catalyst. Chen et al. [5] suggested that at low temperature, not only do the catalysts have poor activities, but also the selectivity of ethylene is low due to a large amount of ethanol that was converted to diethyl ether product. In this research, the reaction temperature of 350°C was selected as the optimum temperature.

Effect of Preparation Methods. In order to investigate the influence of preparation methods on ethanol dehydration, alumina synthesized by solvothermal and sol-gel methods as well as commercial catalysts was studied. The conversion of ethanol over all catalysts is presented in Figure 7. The conversion was found to be in the order Al-SV > Al-SG > Al-com. The Al-SV showed the best performance for dehydration, giving complete conversion at 350°C compared to the other ones. From results of NH_3 -TPD analysis, it seems that there is a relationship between the activity and the ratio of weak acid sites to strong acid sites of alumina catalysts. The sample possessing high ratio of weak to strong acid sites exhibited high catalytic performance on dehydration. The higher activity of Al-SV can be attributed to its higher surface area and higher amount surface acid sites, especially the highest ratio of weak/strong acid strength. Similar trend was found by Hosseini and Nikou [17]; catalyst with high surface area exhibited high activity due to more active sites on large surface area directly to be exposed to ethanol reactant. Xin et al. [1] also reported that the ethanol conversion to ethylene is mainly related to the weak to moderate acid site, while the side reaction such as oligomerization, dehydrocyclization, and the reaction producing higher olefin compounds occurred on the strong acid strength.

In addition, it is generally accepted that ethanol dehydration is an acid-catalyzed reaction. Either Brönsted acid site or Lewis acid site is believed to play an important role in catalytic activity. Different reaction mechanisms of ethanol to ethylene involved the acid sites. One ethanol molecule initially adsorbs on the Brönsted acid site of catalyst and then forms an ethoxide surface species. Subsequently, the ethoxide undergoes deprotonation, losing a proton to Brönsted acid site and forming the ethylene product. On the other hand, the reaction between ethoxide and another ethanol molecule yields diethyl ether (side product). These observations deduced the ethylene selectivity mainly contributed to the Brönsted acidic site [1, 36, 37]. In order to support active



SCHEME 1: Proposed different morphology of alumina obtained from the solvothermal and sol-gel methods.

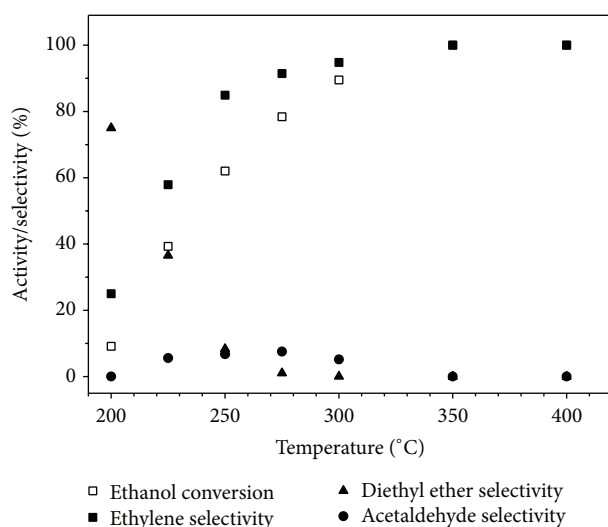


FIGURE 6: Effect of reaction temperature on ethanol conversion and product selectivity over the Al-SV catalyst (reaction condition: $T = 200\text{--}400^\circ\text{C}$, $\text{WHSV} = 8.4 \text{ h}^{-1}$, and catalyst weight = 50 mg).

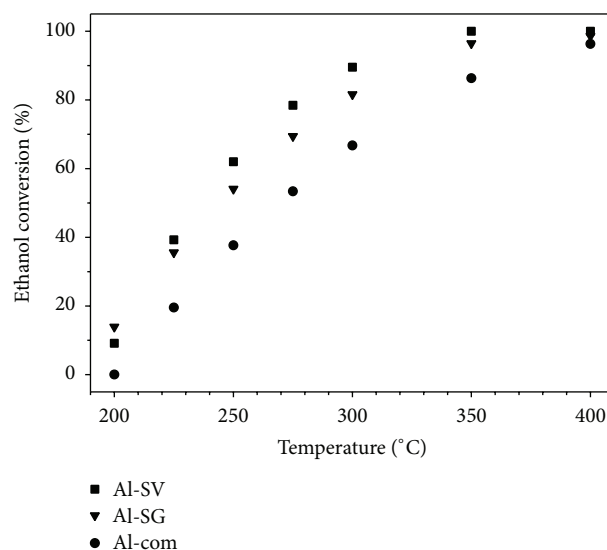


FIGURE 7: The conversion of ethanol over different alumina catalysts (reaction condition: $T = 200\text{--}400^\circ\text{C}$, $\text{WHSV} = 8.4 \text{ h}^{-1}$, and catalyst weight = 50 mg).

Brönsted acidic sites, the dehydration of ethanol over pure siliceous silicate-1 was investigated [1]. They reported that a very low activity with ethanol conversion around 2% was observed. Since the sample consists mainly of Si-OH, there is not Al atom in framework. Therefore, it clearly suggested that the Brönsted acid sites play a crucial role in the ethanol conversion and the formation of ethylene. However, Pan et al. [38] observed the opposite trend with the Lewis acid site. They inferred that the near absence of the acidic Brönsted and the presence of strong Lewis site apparently enhanced the ethylene selectivity. In fact, it should be noted that the $\text{NH}_3\text{-TPD}$ does not provide the nature of surface Brönsted

and Lewis acid site on catalyst surface. Thus, in this study, the types of acidic site (Brönsted or Lewis sites) are not further discussed here. However, it is generally accepted that the ethanol conversion to ethylene occurs on weak acid sites, while the oligomerization and the alcohol transformation to higher hydrocarbon correspond to strong acid strength [39, 40].

From the product selectivity presented in Figures 8, 9, and 10, it was obvious that the Al-SV was able to dehydrate ethanol to ethylene with 100% selectivity, while at 350°C ethylene selectivity was only 87% and 65% for Al-SG and Al-com, respectively. Table 3 summarizes the catalytic ability

TABLE 3: Summary of catalysts for ethylene synthesis and their catalytic ability.

Catalyst	Surface area (m ² /g)	Amount of catalyst	Space velocity (h ⁻¹)	Reaction temperature (°C)	Ethylene yield (%)	References
Al-SV	215	0.05 g	WHSV 8.4	250–350	53–100	This work
H-ZSM-5 (Si/Al = 28)	425	0.2 g	WHSV 0.422	200	9–13	[1]
TiO ₂ /γ-Al ₂ O ₃	187	1.15 mL	LHSV 26–104	360–550	91–99	[5]
Mn-SAPO-34	473	2.0 g	WHSV 2.0	340	97.8	[26]
H ₃ PO ₄ ·12WO ₃ · xH ₂ O	104	10 g	WHSV 1.0	250	68	[27]
Tungstophosphoric acid/MCM-41	183	0.2 g	WHSV 2.9	300	97.9	[28]
P/H-ZSM-5 (Si/Al = 12.18)	160	1.5 g	WHSV 3.0	280–440	31–100	[29]
Ag ₃ PW ₁₂ O ₄₀ ·3H ₂ O	n.a.	0.5 mL	GHSV 6000	220	99.2	[30]
Fe ₂ O ₃	40	10 mL	LHSV 2.85	500	63.4	[31]
Commercial Al ₂ O ₃	190	3.0 mL	LHSV 3.0	450	78.1	[32]
H-ZSM-5 (Si/Al = 25)	295	3.0 mL	LHSV 3.0	450	93.6	[32]

*n.a. = not applicable.

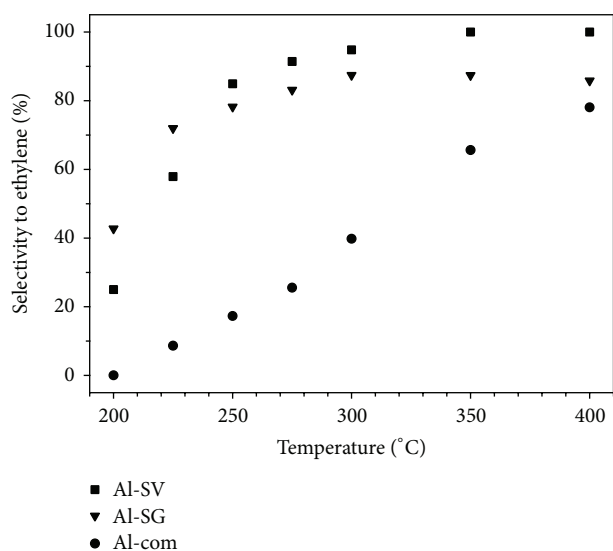


FIGURE 8: The selectivity of ethylene over different alumina catalysts (reaction condition: $T = 200\text{--}400^\circ\text{C}$, $\text{WHSV} = 8.4\text{ h}^{-1}$, and catalyst weight = 50 mg).

for ethanol dehydration to ethylene over various catalysts reported so far. It was obvious that Al-SV is comparable to those of typical and modified catalysts. Thus, the Al-SV is expected to be applied for the ethanol dehydration to ethylene.

To study the amount of coke deposition on catalyst after reaction, TGA measurement was performed. As seen in Figure 11, the weight loss below 150°C was attributed to the removal of physically adsorbed water. The weight loss at higher temperature ($200\text{--}800^\circ\text{C}$) was attributed to the burning of coke deposited on the used sample surface. It was observed that the amount of coke present on various catalysts was in the order of Al-SV (4.0 wt.%) > Al-SG (3.9 wt.%) > Al-com (2.6 wt.%), corresponding to the amount of acidity as determined by $\text{NH}_3\text{-TPD}$ analysis.

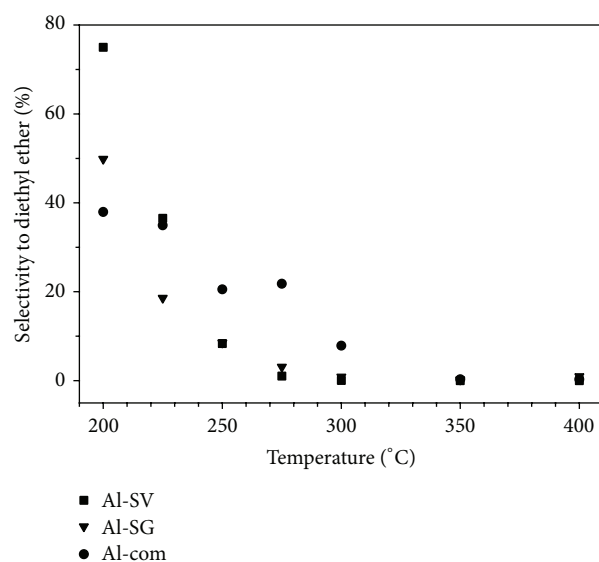


FIGURE 9: The selectivity of diethyl ether over different alumina catalysts (reaction condition: $T = 200\text{--}400^\circ\text{C}$, $\text{WHSV} = 8.4\text{ h}^{-1}$, and catalyst weight = 50 mg).

Accordingly, the textural and acidic properties, the amount of acidic sites, and distribution of acid strength as well as the reaction temperature are important parameters that influenced the catalytic activity. It is thus recommended that alumina catalyst prepared by solvothermal method (Al-SV) was the most suitable catalyst for using in the production of ethylene from ethanol and 350°C was selected as the optimum temperature.

In addition, we extend our study on how the Fe-modified alumina catalyst affects the catalytic activity for ethanol dehydration. We selected solvothermal alumina impregnated with Fe as a catalyst and denoted it as Fe/Al-SV.

The XRD pattern exhibited the presence of Fe characterized by peaks at 24° , 33° , 35.5° , 49° , 54° , and 62° . The average crystallite size calculated by Scherrer equation was 4.43 nm.

TABLE 4: NH_3 -TPD data and catalytic activity of Fe-modified alumina catalyst.

Sample	Number of acid sites ($\mu\text{mol NH}_3/\text{g catalyst}$)		Ethanol conversion ^a (%)	Selectivity ^a (%)		
	Weak to moderate	Strong		Ethylene	Diethyl ether	Acetaldehyde
Al-SV	360	441	100.0	100.0	0.0	0.0
Fe/Al-SV	281	1147	75.2	45.6	2.1	52.3

^a $T = 350^\circ\text{C}$, $P = 1 \text{ atm}$.

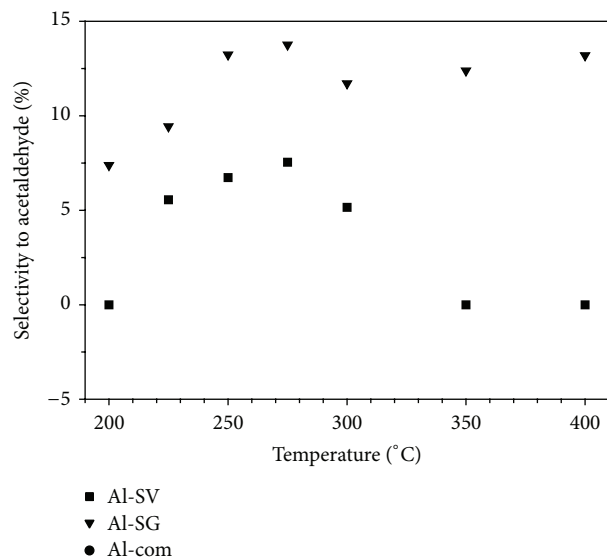


FIGURE 10: The selectivity of acetaldehyde over different alumina catalysts (reaction condition: $T = 200\text{--}400^\circ\text{C}$, $\text{WHSV} = 8.4 \text{ h}^{-1}$, and catalyst weight = 50 mg).

The crystallite size increased after modified with Fe. For the BET surface areas, it can be observed that the addition of Fe leads to a decrease in the surface area. The result changes from 215 to 145 m^2/g , which is due to the pore blockage with Fe. It is consistent with pore size distribution results that it showed a slight shift of pore diameter to small size obtained for Fe/Al-SV.

For NH_3 -TPD results, after the introduction of Fe onto alumina catalyst, the first peak of NH_3 -TPD slightly shifted to higher temperature, while the second peak became broader. It suggested that the weak to moderate acid sites were decreased, but the amount of strong acid strength was increased. The results were probably due to the changes made by alternation of some strong acidic sites to the weak to moderate ones in modified catalysts [20]. A similar result was carried out by Li et al. [41], which reported that the presence of Mn^{4+} in molecular sieve catalyst caused the higher strong acidity, but lower weak acid site.

Table 4 displays the catalytic dehydration of Al-SV and Fe/Al-SV catalysts under the optimized reaction temperature ($T = 350^\circ\text{C}$). It is evident that the activity of Al-SV is higher than Fe-modified catalyst, which is in good agreement with the results of N_2 adsorption-desorption and NH_3 -TPD techniques. The Al-SV has high surface area and possesses large amount of weak to moderate acid sites. This shows

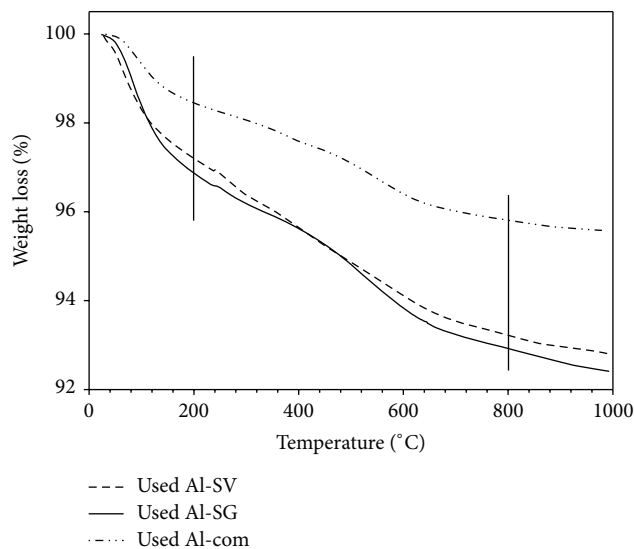
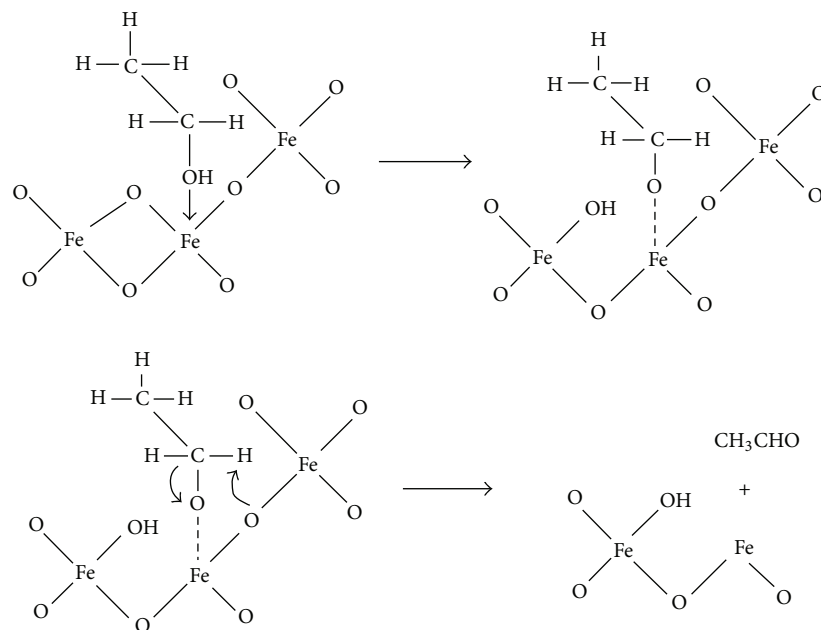


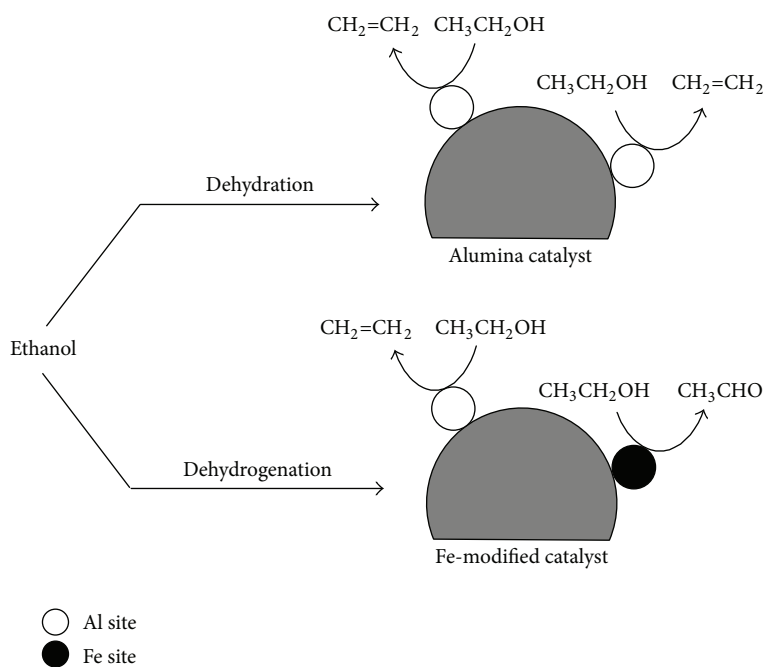
FIGURE 11: TGA curves of the different alumina catalysts.

the importance of textural property and distribution of acid sites as well as the amount of acid site in catalysts. Interestingly, the Fe/Al-SV showed higher selectivity to acetaldehyde compared to unmodified one. An improvement in acetaldehyde selectivity is related to the dehydrogenation pathway promoted by Fe. According to the work done by Li et al. [41], they found that the formation of acetaldehyde over $\text{MnO}_x/\text{molecular sieve}$ catalyst involves (i) the adsorption of ethanol on manganese cations as Lewis acid sites forming ethoxide species; (ii) hydrogen atom of ethoxide abstraction by lattice oxygen and forming acetaldehyde product; (iii) a reoxidation process at metal site and the replenishment of lattice oxygen vacancies to complete catalytic cycle. Also, Michorczyk et al. [42] revealed that the dehydrogenation of propane proceeded via oxidative pathway over catalyst. Propane is oxidized to propene by lattice oxygen from the iron oxide phase (Fe_2O_3 or Fe_3O_4). However, in the oxygen-free experiment, acetaldehyde was found to a small extent because of the limited supply of oxygen. Based on these results and previous studies, a plausible reaction for the formation of acetaldehyde is proposed in Scheme 2.

Although the addition of Fe decreased the ethylene selectivity, the enhanced selectivity to acetaldehyde, which is a valuable compound in petrochemical industry, was obtained. The results in this research suggested a new chance to produce acetaldehyde. The ethanol reaction on alumina catalyst with and without Fe modification is demonstrated in Scheme 3.



SCHEME 2: Proposed reaction for acetaldehyde formation over Fe-modified catalyst.



SCHEME 3: Ethanol reaction over different active sites.

4. Conclusion

The catalytic performance for ethanol dehydration over alumina catalysts prepared by solvothermal and sol-gel methods as well as commercial catalyst was investigated. It revealed that solvothermal-derived alumina showed the highest catalytic activity among other ones because it has the highest surface area and highest ratio of weak acid sites to strong acid sites. From N_2 adsorption-desorption and NH_3 -TPD results, it can be concluded that these textural and

acidic properties significantly affect catalytic dehydration. In addition, in the part of Fe modification, the Fe loading was found to improve the acetaldehyde selectivity. It is due to the ethanol dehydrogenation over Fe species.

Conflict of Interests

The authors declare that there is no conflict of interests regarding the publication of this paper.

Acknowledgments

The authors thank the Thailand Research Fund (BRG5780009 and IRG5780014), National Research University Project, Ratchadaphiseksomphot Endowment Fund (2015) of CU (CU-58-027-AM), and the National Research Council of Thailand (NRCT) for the financial support of this project. They also would like to thank Postdoctoral Scholarship for supporting this research.

References

- [1] H. Xin, X. Li, Y. Fang et al., "Catalytic dehydration of ethanol over post-treated ZSM-5 zeolites," *Journal of Catalysis*, vol. 312, pp. 204–215, 2014.
- [2] E. Aghaei and M. Haghghi, "Effect of crystallization time on properties and catalytic performance of nanostructured SAPO-34 molecular sieve synthesized at high temperatures for conversion of methanol to light olefins," *Powder Technology*, vol. 269, pp. 358–370, 2015.
- [3] K. Ramesh, L. M. Hui, Y.-F. Han, and A. Borgna, "Structure and reactivity of phosphorous modified H-ZSM-5 catalysts for ethanol dehydration," *Catalysis Communications*, vol. 10, no. 5, pp. 567–571, 2009.
- [4] D. Varisli, T. Dogu, and G. Dogu, "Ethylene and diethyl-ether production by dehydration reaction of ethanol over different heteropolyacid catalysts," *Chemical Engineering Science*, vol. 62, no. 18–20, pp. 5349–5352, 2007.
- [5] G. Chen, S. Li, F. Jiao, and Q. Yuan, "Catalytic dehydration of bioethanol to ethylene over $\text{TiO}_2/\gamma\text{-Al}_2\text{O}_3$ catalysts in micro-channel reactors," *Catalysis Today*, vol. 125, no. 1–2, pp. 111–119, 2007.
- [6] L.-P. Wu, X.-J. Li, Z.-H. Yuan, and Y. Chen, "The fabrication of TiO_2 -supported zeolite with core/shell heterostructure for ethanol dehydration to ethylene," *Catalysis Communications*, vol. 11, no. 1, pp. 67–70, 2009.
- [7] M. Mokhtar, S. N. Basahel, and T. T. Ali, "Ethanol to hydrocarbons using silver substituted polyoxometalates: physicochemical and catalytic study," *Journal of Industrial and Engineering Chemistry*, vol. 20, no. 1, pp. 46–53, 2014.
- [8] J. Bi, X. Guo, M. Liu, and X. Wang, "High effective dehydration of bio-ethanol into ethylene over nanoscale HZSM-5 zeolite catalysts," *Catalysis Today*, vol. 149, no. 1–2, pp. 143–147, 2010.
- [9] Y. Han, C. Lu, D. Xu, Y. Zhang, Y. Hu, and H. Huang, "Molybdenum oxide modified HZSM-5 catalyst: surface acidity and catalytic performance for the dehydration of aqueous ethanol," *Applied Catalysis A: General*, vol. 396, no. 1–2, pp. 8–13, 2011.
- [10] E. A. El-Katatny, S. A. Halawy, M. A. Mohamed, and M. I. Zaki, "Recovery of ethene-selective $\text{FeO}_x/\text{Al}_2\text{O}_3$ ethanol dehydration catalyst from industrial chemical wastes," *Applied Catalysis A: General*, vol. 199, no. 1, pp. 83–92, 2000.
- [11] S. Alamolhoda, M. Kazemeini, A. Zaherian, and M. R. Zakerinasab, "Reaction kinetics determination and neural networks modeling of methanol dehydration over nano $\gamma\text{-Al}_2\text{O}_3$ catalyst," *Journal of Industrial and Engineering Chemistry*, vol. 18, no. 6, pp. 2059–2068, 2012.
- [12] Y. Matsumura, K. Hashimoto, and S. Yoshida, "Selective dehydrogenation of ethanol over highly dehydrated silica," *Journal of Catalysis*, vol. 117, no. 1, pp. 135–143, 1989.
- [13] R. Takahashi, S. Sato, T. Sodesawa, K. Arai, and M. Yabuki, "Effect of diffusion in catalytic dehydration of alcohol over silica-alumina with continuous macropores," *Journal of Catalysis*, vol. 229, no. 1, pp. 24–29, 2005.
- [14] A. T. Aguayo, A. G. Gayubo, A. Atutxa, M. Olazar, and J. Bilbao, "Catalyst deactivation by coke in the transformation of aqueous ethanol into hydrocarbons. Kinetic modeling and acidity deterioration of the catalyst," *Industrial & Engineering Chemistry Research*, vol. 41, no. 17, pp. 4216–4224, 2002.
- [15] Q. Sheng, K. Ling, Z. Li, and L. Zhao, "Effect of steam treatment on catalytic performance of HZSM-5 catalyst for ethanol dehydration to ethylene," *Fuel Processing Technology*, vol. 110, pp. 73–78, 2013.
- [16] G. Moradi, F. Yaripour, H. Abbasian, and M. Rahmanzadeh, "Intrinsic reaction rate and the effects of operating conditions in dimethyl ether synthesis from methanol dehydration," *Korean Journal of Chemical Engineering*, vol. 27, no. 5, pp. 1435–1440, 2010.
- [17] S. Y. Hosseini and M. R. K. Nikou, "Investigation of different precipitating agents effects on performance of $\gamma\text{-Al}_2\text{O}_3$ nanocatalysts for methanol dehydration to dimethyl ether," *Journal of Industrial and Engineering Chemistry*, vol. 20, no. 6, pp. 4421–4428, 2014.
- [18] S. S. Akarmazyan, P. Panagiotopoulou, A. Kambolis, C. Papadopoulou, and D. I. Kondarides, "Methanol dehydration to dimethylether over Al_2O_3 catalysts," *Applied Catalysis B: Environmental*, vol. 145, pp. 136–148, 2014.
- [19] D. Liu, C. Yao, J. Zhang, D. Fang, and D. Chen, "Catalytic dehydration of methanol to dimethyl ether over modified $\gamma\text{-Al}_2\text{O}_3$ catalyst," *Fuel*, vol. 90, no. 5, pp. 1738–1742, 2011.
- [20] F. Yaripour, Z. Shariatnia, S. Sahebdehfar, and A. Irandoukht, "The effects of synthesis operation conditions on the properties of modified γ -alumina nanocatalysts in methanol dehydration to dimethyl ether using factorial experimental design," *Fuel*, vol. 139, pp. 40–50, 2015.
- [21] G. Moretti, G. Fierro, G. Ferraris, G. B. Andreozzi, and V. Naticchioni, " N_2O decomposition over [Fe]-MFI catalysts: influence of the Fe_xO_y nuclearity and the presence of framework aluminum on the catalytic activity," *Journal of Catalysis*, vol. 318, pp. 1–13, 2014.
- [22] K. Aasberg-Petersen, I. Dybkjær, C. V. Ovesen, N. C. Schjødt, J. Sehested, and S. G. Thomsen, "Natural gas to synthesis gas—catalysts and catalytic processes," *Journal of Natural Gas Science and Engineering*, vol. 3, no. 2, pp. 423–459, 2011.
- [23] J. Pérez-Ramírez and A. Gallardo-Llamas, "Impact of the preparation method and iron impurities in Fe-ZSM-5 zeolites for propylene production via oxidative dehydrogenation of propane with N_2O ," *Applied Catalysis A: General*, vol. 279, no. 1–2, pp. 117–123, 2005.
- [24] M. S. M. Yusoff and M. Muslimin, "Synthesis of alumina using the solvothermal method," *Malaysian Journal of Analytical Sciences*, vol. 11, no. 1, pp. 262–268, 2007.
- [25] S. Saha, "Preparation of alumina by sol-gel process, its structures and properties," *Journal of Sol-Gel Science and Technology*, vol. 3, no. 2, pp. 117–126, 1994.
- [26] Y. Chen, Y. Wu, L. Tao et al., "Dehydration reaction of bio-ethanol to ethylene over modified SAPO catalysts," *Journal of Industrial and Engineering Chemistry*, vol. 16, no. 5, pp. 717–722, 2010.
- [27] V. V. Bokade and G. D. Yadav, "Heteropolyacid supported on montmorillonite catalyst for dehydration of dilute bio-ethanol," *Applied Clay Science*, vol. 53, no. 2, pp. 263–271, 2011.
- [28] A. Ciftci, D. Varisli, K. Cem Tokay, N. Asli Sezgi, and T. Dogu, "Dimethyl ether, diethyl ether & ethylene from alcohols over

- tungstophosphoric acid based mesoporous catalysts,” *Chemical Engineering Journal*, vol. 207–208, pp. 85–93, 2012.
- [29] D. Zhang, R. Wang, and X. Yang, “Effect of P content on the catalytic performance of P-modified HZSM-5 catalysts in dehydration of ethanol to ethylene,” *Catalysis Letters*, vol. 124, no. 3–4, pp. 384–391, 2008.
- [30] J. Gurgul, M. Zimowska, D. Mucha, R. P. Socha, and L. Matachowski, “The influence of surface composition of $\text{Ag}_3\text{PW}_{12}\text{O}_{40}$ and $\text{Ag}_3\text{PMo}_{12}\text{O}_{40}$ salts on their catalytic activity in dehydration of ethanol,” *Journal of Molecular Catalysis A: Chemical*, vol. 351, pp. 1–10, 2011.
- [31] T. Zaki, “Catalytic dehydration of ethanol using transition metal oxide catalysts,” *Journal of Colloid and Interface Science*, vol. 284, no. 2, pp. 606–613, 2005.
- [32] X. Zhang, R. Wang, X. Yang, and F. Zhang, “Comparison of four catalysts in the catalytic dehydration of ethanol to ethylene,” *Microporous and Mesoporous Materials*, vol. 116, no. 1–3, pp. 210–215, 2008.
- [33] J. Khom-in, P. Praserttham, J. Panpranot, and O. Mekasuwandumrong, “Dehydration of methanol to dimethyl ether over nanocrystalline Al_2O_3 with mixed γ - and χ -crystalline phases,” *Catalysis Communications*, vol. 9, no. 10, pp. 1955–1958, 2008.
- [34] G. Leofanti, M. Padovan, G. Tozzola, and B. Venturelli, “Surface area and pore texture of catalysts,” *Catalysis Today*, vol. 41, no. 1–3, pp. 207–219, 1998.
- [35] X. Liu, W.-Z. Lang, L.-L. Long, C.-L. Hu, L.-F. Chu, and Y.-J. Guo, “Improved catalytic performance in propane dehydrogenation of $\text{PtSn}/\gamma\text{-Al}_2\text{O}_3$ catalysts by doping indium,” *Chemical Engineering Journal*, vol. 247, pp. 183–192, 2014.
- [36] W. R. Moser, R. W. Thompson, C.-C. Chiang, and H. Tong, “Silicon-rich H-ZSM-5 catalyzed conversion of aqueous ethanol to ethylene,” *Journal of Catalysis*, vol. 117, no. 1, pp. 19–32, 1989.
- [37] L. Silvester, J.-F. Lamonier, J. Faye et al., “Reactivity of ethanol over hydroxyapatite-based Ca-enriched catalysts with various carbonate contents,” *Catalysis Science & Technology*, vol. 5, pp. 2994–3006, 2015.
- [38] Q. Pan, A. Ramanathan, W. Kirk Snavely, R. V. Chaudhari, and B. Subramaniam, “Intrinsic kinetics of ethanol dehydration over Lewis acidic ordered mesoporous silicate, Zr-KIT-6,” *Topics in Catalysis*, vol. 57, pp. 1407–1411, 2014.
- [39] K. K. Ramasamy and Y. Wang, “Catalyst activity comparison of alcohols over zeolites,” *Journal of Energy Chemistry*, vol. 22, no. 1, pp. 65–71, 2013.
- [40] M. Zhang and Y. Yu, “Dehydration of ethanol to ethylene,” *Industrial & Engineering Chemistry Research*, vol. 52, no. 28, pp. 9505–9514, 2013.
- [41] J. Li, R. Wang, and J. Hao, “Role of lattice oxygen and lewis acid on ethanol oxidation over OMS-2 catalyst,” *The Journal of Physical Chemistry C*, vol. 114, no. 23, pp. 10544–10550, 2010.
- [42] P. Michorczyk, P. Kuśtrowski, L. Chmielarz, and J. Ogonowski, “Influence of redox properties on the activity of iron oxide catalysts in dehydrogenation of propane with CO_2 ,” *Reaction Kinetics and Catalysis Letters*, vol. 82, no. 1, pp. 121–130, 2004.



Hindawi

Submit your manuscripts at
<http://www.hindawi.com>

